Available online at www.sciencedirect.com

ScienceDirect

Energy Procedia 49 (2014) 2118 – 2124

Energy Procedia

SolarPACES 2013

Model based open-loop correction of heliostat tracking errors

K. Malan [a]* and P. Gauché [a]

[a] Solar Thermal Energy Research Group, Dept. of Mechanical and Mechatronic Engineering, Stellenbosch University, 7602, South Africa

Abstract

The heliostat field is by far the most expensive part of a typical Central Receiver (CR) plant. To achieve high conversion efficiencies, heliostats with very high tracking accuracy are needed, but errors are introduced due to manufacturing-, installation- and alignment tolerances as well control system granularity. Mechanical error profiles are unique for every heliostat and cause tracking errors that vary over the course of days and seasons and therefore cannot be corrected by once-off angle offset corrections. Developments in microcontroller technology drives decentralization of CR control systems. Powerful open-loop error correction algorithms can run on low cost heliostat local controllers, enabling high tracking accuracy from lower cost heliostats with reduced tolerances.

A prototype array of 18 heliostats, each 1 ft^2 in size, was constructed to validate the field control system functionality and final tracking accuracy. Tests were conducted at SU's solar laboratory with an 18m tower and heliostat slant ranges of around 40 m.

Prototype experiments indicate a daily open-loop RMS normal vector tracking error below 1 mrad. Strong correlation exists between successive days' residual error curves, indicating that further model refinements may be possible, including frequency spectrum analysis (using FFT) to identify and correct for mechanism-specific periodic drivetrain errors.

Selection and peer review by the scientific conference committee of SolarPACES 2013 under responsibility of PSE AG.
Final manuscript published as received without editorial corrections.
Keywords: Central receiver; heliostat tracking; error correction; control systems

* Corresponding author. Tel.: +27 (0)21 808 4016.
E-mail address: karelmalan@gmail.com / karel@sun.ac.za.

Selection and peer review by the scientific conference committee of SolarPACES 2013 under responsibility of PSE AG.
Final manuscript published as received without editorial corrections.
doi:10.1016/j.egypro.2014.03.224

1. Introduction

The long term economic feasibility of concentrating solar power (CSP) is dependent on efforts to reduce system cost while increasing overall energy conversion efficiency. Since the heliostat field typically makes up 40-50% of central receiver (CR) CAPEX [1], it makes sense to develop control methods that would allow low cost heliostats to operate with very high tracking accuracies. The US Department of Energy's Sunshot Initiative identifies heliostat tracking as one of the areas of research to be pursued to reduce CSP's levellised cost of electricity (LCOE) to below 6¢ per kWh by 2020. The aim of model based tracking correction methods is to individually characterize the movement of every heliostat in the system so that real time, open loop correction of deterministic tracking errors may be performed for all possible solar angles without the need for any feedback from the target, except for periodic updating of calibration coefficients by means of scheduled measurements of individual heliostat beam errors.

Baheti and Scott [2] first developed a model based heliostat error correction method in the late 1970's to compensate for mechanical errors inherent in typical heliostat mechanisms. This model included pedestal tilt, azimuth- and elevation bias offsets, drive wheel radius errors and non-orthogonal drive axes. A closed-loop sun sensor was used to periodically point the heliostat normal vector directly at the sun. Heliostat pointing errors were obtained by comparing the commanded heliostat position at each interval with the actual solar position as calculated by solar algorithm. This data was used to estimate coefficients for the error model and resulted in final RMS error reductions of 10:1 and 5:1 for azimuth- and elevation tracking respectively. This and other model-based methods were initially not widely implemented due to the high cost and practical constraints of computers at the time.

A subsequent heliostat tracking model was patented in 1986 by Kenneth Stone [3] which added the effects of non-orthogonal drive axes to those of [2]. The effect of gravity sag was also later added in a generalized model [4]. This method has since been widely cited and can be considered the basis for model based open-loop heliostat error correction since. Stone and Jones [5] demonstrated the time varying nature of individual heliostat error sources in an analysis of tracking errors at Solar Two.

Recently, an updated method was described by Khalsa, Ho and Andraka [6] which added two new error sources to that of [2]. Non-orthogonal drive axes is accounted for by a first order approximation of azimuth error. The resulting azimuth adjustment term is expressed as a function of the non-orthogonality angle and input elevation angle. The effect of boresight errors are also handled by an azimuth adjustment term, while the elevation component forms part of the bias adjustment term.

An automatic method for getting feedback information of heliostat tracking error offsets on a calibration target was developed at Solar One [7]. More recently, Berenguel *et al.* [8] described an automated angle offset correction method with detailed image processing techniques for finding calibration target edge markers for image perspective correction and heliostat beam offset calculation.

This paper describes the development of a scalable, modular and adaptable control system aimed at low cost heliostats deployed on rough, non-flat terrain without the need for accurate surveying of installed locations or precision structure leveling during installation. This research fits in with the Stellenbosch University solar power thermodynamic cycle (SUNSPOT) concept [9] which requires a high solar concentration ratio to drive a gas turbine in the primary loop.

Our error correction method is based on the work done by [2] and [3] in the 1980's and recently [6]. The error model described here differs from that of [6] in that it includes a translation step to account for heliostat location uncertainty. This fits in with our aim of correcting tracking errors associated with very low installation- and manufacturing tolerances. Also, boresight errors are not handled explicitly, instead being accounted for by bias angle offsets. The model produces 2D error offset positions representing reflected beam intersection points on a plane perpendicular to the heliostat-to-target vector instead of heliostat normal vector offset angles as is used in most other models. This allows a step by step, intuitive approach to the model, but may need to be optimized in future.

The following sections describe the error model and correction method and give an overview of the prototype system layout and the distributed processing and networking strategy. Finally, tracking results obtained from field tests are presented and discussed.

2. Prototype system

A prototype array consisting of 18 heliostats, each with $1 ft^2$ of mirror surface was constructed to test the overall system architecture and to validate the error model. The heliostat mechanisms were designed to be constructed using low tolerance laser cut and bent steel plate sections with the aim of being highly adjustable bolted assemblies requiring no machining or welding. The resulting random mechanical error profiles typically introduced during each mechanism's assembly presented a challenge for the tracking- and error correction system. Figure 1 gives a representation of the high level system components.

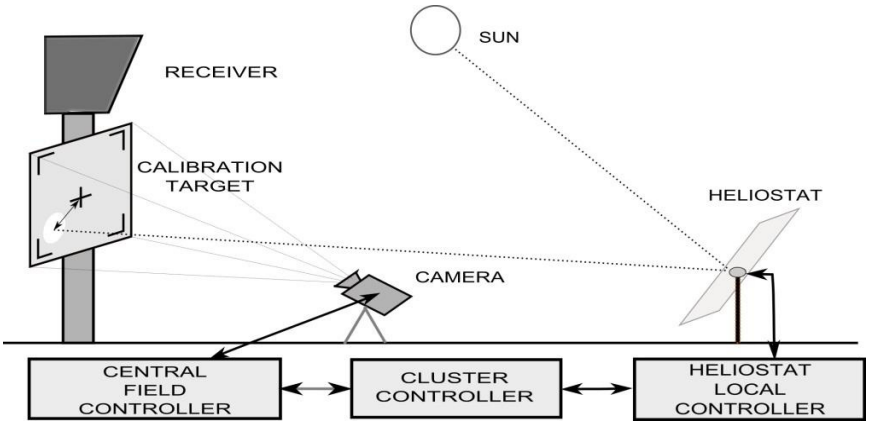

Figure 1: Prototype system layout

2.1 Concept of operation

A camera based method with calibration target and image processing techniques similar to [8] are used to periodically determine individual heliostats' tracking error offsets. These offsets are used to estimate error model coefficients of each heliostat. By using these heliostat-specific coefficients and applying the error model in reverse, real time tracking error estimation and correction is performed by each heliostat's local controller unit.

2.2 Distributed processing and communication

Recent trends in CR control indicate a decentralization of processing tasks [10]. Our system's tasks are distributed among three distinct processing tiers according to the required processing resources and frequency of execution. Real time tasks were moved down the hierarchy to the cluster- and local controllers to free up processing resources in- and bandwidth to the central controller.

The central controller forms the topmost processing tier and hosts a graphical user interface which allows monitoring and adjustment of all system parameters and individual heliostats' tracking mode, orientation and a complete set of location- and error parameters specific to each unit.

Heliostats are grouped into semi-autonomous clusters, each of which fall under the supervision of a cluster controller (CC). The CC units form the middle processing tier. Each CC is responsible for calculating the solar position vector using an embedded solar algorithm [11], with time and date supplied by its own GPS unit. Once every second, solar position data is broadcast to all heliostats in the cluster. The CC is also responsible for collating status information from all heliostats in its group and so acts as a communication multiplexer between the central controller and the multitude of heliostat local controllers below it. This configuration means that each heliostat cluster operates as a semi-autonomous unit, only needing configuration data at startup and occasional heartbeat messages thereafter from the central controller to ensure continued safe operation. Since each cluster handles all its own real time processing and communication requirements, scaling up the number of heliostats can be achieved by

simply adding more clusters without needing significant extra bandwidth or processing resources from the rest of the system.

Each heliostat's local controller (LC) stores its location, aim point, current step counts, error coefficients and operating mode in local memory. For each new set of incoming solar angles, it calculates the ideal heliostat normal vector, applies the error model correction steps and translates this into control commands for the motor drivers.

3. Model based error correction

A model is derived to predict a generic heliostat's reflected beam error offset 'signature' on the target plane as a function of its position relative to the tower, the input solar vector set and the set of coefficients which describe the heliostat error geometry.

3.1 Model derivation

A step by step derivation is shown for azimuth-elevation heliostats. An entire set of solar angles corresponding to beam error measurement times are normally used as input to the model. For the sake of brevity, we write $\hat{x}_{\mathrm{i}}$ to indicate the i[th] vector in a set $\hat{x}_{1..\mathrm{n}}$ of vectors for each step below.

a. For each input solar vector $\hat{s}_{\mathrm{i}}$, calculate the ideal heliostat normal unit vector $\hat{h}_{ideal,i}$ as derived in [12].

b. Add elevation- and azimuth bias angles (α_{bias} and θ_{bias} respectively) to the ideal heliostat normal vector:

$$\alpha_{\mathrm{Hb,i}} = \alpha_{\mathrm{H,i}} + \alpha_{\mathrm{bias}} \tag{1}$$

$$\theta_{\mathrm{Hb,i}} = \theta_{\mathrm{H,i}} + \theta_{\mathrm{bias}} \tag{2}$$

c. Add non-orthogonal drive axes error by adding a first-order approximation of the resulting azimuthal error $\Delta\theta_i = \psi_{\mathrm{no}}.\tan(\alpha_{\mathrm{Hb,i}})$ as derived in [8] to yield bias- and non-orthogonality adjusted normal vector:

$$\hat{h}_{bno,i} = \left[\sin(\alpha_{\mathrm{Hb,i}}) \quad \cos(\alpha_{\mathrm{Hb},i})\sin(\theta_{\mathrm{Hb},i} + \Delta\theta_i) \quad \cos(\alpha_{\mathrm{Hb},i})\cos(\theta_{\mathrm{Hb},i} + \Delta\theta_i)\right] \tag{3}$$

d. Find the final error-adjusted heliostat normal vector $\hat{h}_{adj,i}$ by adding the effect of pedestal tilt as follows:

$$\hat{h}_{adj,i} = R_N(\gamma_N)R_E(\gamma_E)\hat{h}_{bno,i} \tag{4}$$

where and $R_N(\gamma_N)$ and $R_E(\gamma_E)$ are rotation matrices with rotation direction corresponding to the right-hand rule convention.

e. Substitute the ideal heliostat normal vector set of (a) with the adjusted vector set of (d). The adjusted heliostat-to-target vector set $\hat{t}_{adj,i}$ is then given by:

$$\hat{t}_{adj,\mathrm{i}} = \hat{h}_{adj,i} \,.\, 2\cos(\phi_{adj,i}) - \hat{s}_i \tag{5}$$

$$\text{with } \phi_{adj,i} = \cos^{-1}(\hat{s}_i \cdot \hat{h}_{adj,i}) \tag{6}$$

where $\phi_{adj,i}$ is the combined error-adjusted incidence angle corresponding to the input solar angle $\hat{s}_i$.

f. Translate the heliostat-to-target vector by $\mathrm{T}[\Delta_{\mathrm{Z}}, \Delta_{\mathrm{E}}, \Delta_{\mathrm{N}}]$ to account for heliostat location error and yield the real heliostat location B_{real}.

g. Construct a target plane perpendicular to the heliostat-to-target vector $\hat{N}$ and passing through the target center.

$$d = -\hat{N} \cdot [A]' \tag{7}$$

where B is the heliostat location, A the target location and $\hat{N} = A - B$.

The adjusted heliostat-to-target vector set ($\hat{t}_{adj,i}$) is added to the translated heliostat position (B_{real}) to find a set of reflected solar image positions ($P_{1..n}$) which will intersect with the target plane when solving for

$$u = \frac{(N \cdot B_{real}) + d}{N \cdot (B_{real} - P_{1..n})} \tag{8}$$

This yields a set of intersection points on the target plane, given by

$$P_{int,1..n} = +u.(P_{1..n} - B_{real}) \tag{9}$$

The set of intersection points is translated to lie around the origin and rotated to lie on the vertical East-West plane for convenient extraction of two dimensional X- and Y offsets on the target plane which form the error model outputs.

3.2 Estimation of error coefficients

A diagram of the procedure for estimating an eight-dimensional error coefficient vector X_8 is shown in Figure 2. An iterative method was implemented in Matlab. It takes as input the heliostat's location, the current error vector $X_{8,i}$ and a set of solar angles corresponding to measured error timestamps. From these inputs, the error model produces a set of predicted error offsets on the calibration target. During each iteration of the algorithm, the current error vector is updated by means of the Nelder-Mead simplex optimization algorithm until certain termination conditions are met. In our case, the conditions are met after a predetermined number of iterations or when the RMS error between the sets of predicted- and measured error offsets is sufficiently small.

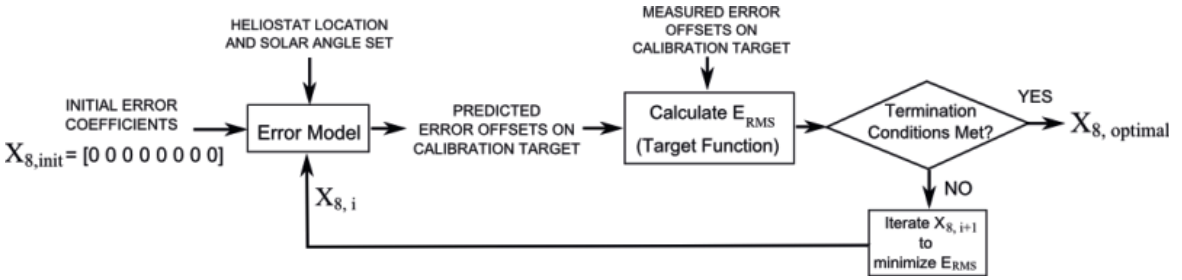

Figure 2: Error coefficient estimation procedure

4. Results

Tracking accuracy measurements were performed using the prototype system described earlier, a photograph of which is shown in Figure 3. The system was deployed on the solar roof laboratory at the Department of Mechanical and Mechatronic Engineering at Stellenbosch University. The overall functionality of the array control system was evaluated and measurements were taken of daily tracking accuracy on a calibration target located 4m below the nominal receiver aim point. Figure 3 shows a photograph of the prototype system.

Figure 3: The solar lab test setup, showing a number of small prototype heliostats on mounting platforms.

Figure 4 shows open loop tracking data for three consecutive days by heliostat unit A3, located 30.8 m South and 19.2 m East of the tower and with a slant range of roughly 37.5 m. Table 1 shows the set of error coefficients predicted by the coefficient estimation algorithm.

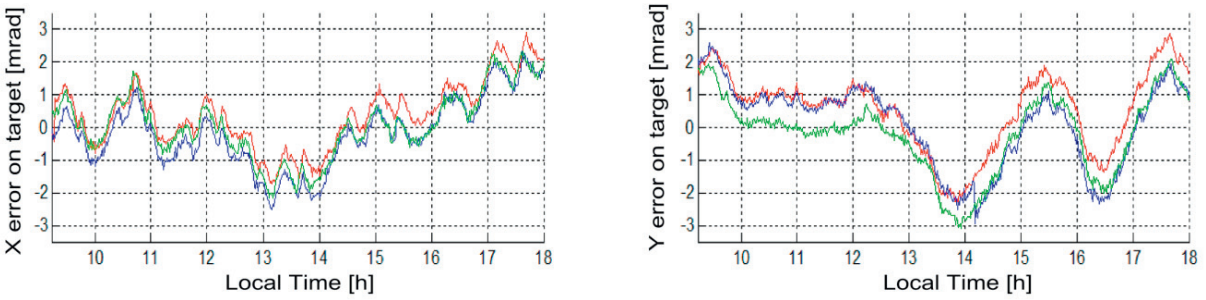

Figure 4: On-target tracking results for three consecutive days. 2012-08-06 (red), 2012-08-07 (blue), 2012-08-08 (green).

Table 1: Heliostat Error Coefficient Values

Location translation [m]			Pedestal tilt [mrad]		Axes Non-Orthogonality [mrad]	Bias Angles [mrad]	
Δ_N	Δ_E	Δ_Z	γ_N	γ_E	ψ_{no}		
-0.53	1.02	0.06	-13.27	9.56	-1.92	-3.79	1.12

These values were used by the heliostat local controller to calculate the adjusted normal angles which led to the daily tracking performances shown in Figure 4 (three consecutive days). The daily RMS error for 2012-08-06 was 1.97 mrad on the calibration target, which translates to just under one mrad for the heliostat normal vector.

These tracking results clearly demonstrates day to day repeatability and suggests that residual tracking errors are deterministic in nature. Overall accuracy may be further improved by refinement of the model to include drivetrain specific error sources.

5. Conclusion

The development of a modular, scalable and highly flexible heliostat control architecture using a model based tracking error correction method was described and validated experimentally.

A Sasol funded project is underway to develop a 40m^2 heliostat array which will be located on the solar roof laboratory at Mechanical Engineering, Stellenbosch University. The heliostat tracking error model is being expanded to incorporate linear actuator driven fixed horizontal heliostats and azimuth elevation heliostats with slew driven azimuth axis and linear actuator driven elevation axis. Work is underway to model the residual tracking errors (figure 4) as deterministic drivetrain-specific error effects.

Future work requires more experimental data gathered at different times of year. Refinement of the model coefficient estimation algorithm is required to achieve better understanding of sensitivities, as discussed in [13].

Acknowledgements

The authors would like to thank Sasol Technology, the Department of Science and Technology of South Africa through the Solar Thermal Spoke fund and the Stellenbosch University Hope project for funding the resources to perform this work and present it at SolarPACES. Also for the academic support of the Solar Thermal Energy Research Group (STERG).

References

[1] Kolb, G. J., Jones, S. A., Donnelly, M. W., Gorman, D., Thomas, R., Davenport, R., Lumia, R. Heliostat Cost Reduction Study. SAND2007-3293. SANDIA National Laboratories, New Mexico / California. 2007.

[2] Baheti, R. S., Scott, P. F. 1980. Design of Self-calibrating Controllers for Heliostats in a Solar Power Plant. IEEE Transactions on Automatic Control, Vol. AC-25, #6, 1980-Dec.

[3] Stone, K. W. 1986. Automatic Heliostat Track Alignment Method. US Patent 4,564,275 by McDonnell Douglas Corporation.

[4] Stone, K. W., Kiefer, J. A. 1998. Open Loop Track Alignment Methodology. American Solar Energy Society Conference Proceedings. Albuquerque, New Mexico.

[5] Stone, K. W., Jones, S. A. 1999. Analysis of Solar Two Heliostat Tracking Error Sources. Sandia National Laboratories. SAND99-0239.

[6] Khalsa, S. S., Ho, C. K., Andraka, C. E. 2011. An Automated Method to Correct Heliostat Tracking Errors. SolarPACES 2011.

[7] Blackmon, J. B., Caraway, M. J., Iwaki, A., I. 1986. Solar One Beam Characterization System. Sandia Contract 84-8173.

[8] Berenguel, M., Rubio, F. R., Valverde, A., Lara, P. J., Arahal, M. R., Camacho, E. F., Lopez, M., 2003. An Artificial vision-based control system for automatic heliostat positioning offset correction in a central receiver solar power plant. Solar Energy Vol 76, pp563-575.

[9] D. G. Kröger. The Stellenbosch University Solar Power Thermodynamic Cycle. 2011. http://tinyurl.com/qafkw72

[10] Camacho, E. F., Berenguel, M., Rubio, F. R., Martìnez, D. 2012. Advances in Industrial Control: Control of Solar Energy Systems. Springer. ISBN 978-0-85729-915-4.

[11] Grena, R. 2007. An Algorithm for the Computation of the Solar Position. Solar Energy 82 (2008) 462–470. .

[12] Stine, W., Geyer, M. 2001. Power from the Sun. www.powerfromthesun.net

[13] Zhang, J. J., Pye, J. D., Ho, C. K. 2012. Estimation of Uncertainty in Automated Heliostat Alignment. Australian Solar Council Solar 2012 Conference Proceedings. Melbourne.